Chapter 4

The combined effects of Faraday rotation and absorption on the polarization from accretion disk atmospheres

4.1 Introduction

As discussed in chapters 2 and 3, the polarization emerging from accretion disk atmospheres can be affected strongly by either magnetic fields or absorption opacity. However, we did not consider the interplay that might occur when both absorption opacity and Faraday rotation are present. The Faraday rotation calculations of chapter 2 assumed a pure electron scattering atmosphere, but absorption opacity might reduce the depolarization. This is because the Faraday rotation of a given photon depends on the total electron column density that the photon traverses. The dominant effect of Faraday rotation occurs after last scattering, so if the absorption opacity significantly reduces the electron scattering column down to unit optical depth, the depolarization would be smaller. On the other hand, the absorption opacity itself may directly increase or decrease the polarization from an unmagnetized disk, as discussed in chapter 3. In this chapter we attempt to disentangle these effects in order to understand how Faraday rotation and absorption opacity act together to determine the polarization of the radiation emerging from AGN accretion discs. We have

discovered a number of subtle phenomena which are not immediately obvious from the above arguments.

As in chapter 2, we use Monte Carlo calculations of the radiative transfer. However, most of our results are from solving the transfer equation described in section 2.2.2. The emerging radiation field can be calculated much faster using standard finite difference techniques, and we present the results of both approaches in simple toy atmosphere models in section 4.3. In section 4.4 we discuss again the role of Faraday rotation in determining the optical polarization in AGN accretion discs, and we summarize our conclusions in section 4.5.

4.2 Equations and numerical techniques

Chapter 2 describes a Monte Carlo technique to calculate the polarized radiative transfer through a magnetized, pure electron scattering atmosphere. We have modified this slightly to include the effects of absorption opacity κ_ν at frequency ν, assuming for simplicity that the ratio of absorption opacity to electron scattering opacity is independent of optical depth in the atmosphere. In other words,

$$q_\nu \equiv \frac{n_e \sigma_T}{\kappa_\nu + n_e \sigma_T} \tag{4.1}$$

is constant, where n_e is the electron number density and σ_T is the Thomson cross section. We propagate each photon a vertical optical depth $\tau_\nu = \tau_{\nu 0} + \mu \ln(r_1)$ through the atmosphere, where r_1 is a random deviate between 0 and 1, μ is the direction cosine of the photon propagation vector with respect to the upward vertical, and $\tau_{\nu 0}$ is the starting total optical depth. The photon's polarization vector is Faraday rotated according to equation (2.11). Then, another random deviate, r_2, between 0 and 1 is chosen. If r_2 is less than q_ν, the photon is scattered. Otherwise it is absorbed and another photon is started at the base of the atmosphere. This process is repeated until a photon escapes from the atmosphere, and it is binned as described in chapter 2. No thermal emissivity is included in the Monte Carlo calculations.

We also use the equations derived in section 2.2.2 including Faraday rotation, absorption opacity, and a source function. Again, we solve the equations using the Feautrier method. Most of the results presented in this chapter are based on this method since it is speedier (especially when the absorption opacity is large) and more accurate than the Monte Carlo method, and can be used to

study the effects of changing the source function.

4.3 Constant q_ν atmospheres

In order to illuminate the physics, we now consider two idealized atmosphere problems, both with q_ν independent of optical depth. The first case has zero thermal source function everywhere except for a source at infinite optical depth. The second case has an isotropic thermal source function which varies linearly with optical depth. These problems were solved in the unmagnetized case by Loskutov and Sobolev (1979). Photons of different frequency are completely decoupled in our radiative transfer equation for an atmosphere of fixed assumed structure, i.e. there is no frequency redistribution. We therefore drop the subscript ν on all variables and parameters from now on.

4.3.1 Case 1: radiation sources from large optical depth

This problem is a generalization of the pure electron scattering case considered by Chandrasekhar (1960), but it is important to note that the presence of absorption opacity in this case implies that the intensity of the radiation emerging from the top of the atmosphere is formally zero unless there is infinite illumination from below. Nevertheless the radiation field is still polarized. This problem therefore represents an idealization of an atmosphere in which photons of a given frequency are thermally emitted in significant quantities only at large optical depth.

From the numerical standpoint we have performed both the Monte Carlo simulations and the Feautrier calculation using sources at sufficiently high, but finite, optical depth so that the polarization no longer depends on this depth. We apply a lower boundary condition of unpolarized, isotropic radiation sources. The results then depend on only two parameters, δ and q.

Figure 4.1 shows the polarization as a function of viewing angle for a variety of values of q in an unmagnetized atmosphere. The lowest curve shows the pure electron scattering case ($q = 1$). Loskutov and Sobolev (1979) numerically calculated cases for $q > 0.5$, and found that the polarization increased monotonically as q decreased, i.e. absorption opacity increased. Their results are also shown in figure 4.1 and are in excellent agreement with ours. They also found that the polarization should continue to rise for even smaller q, and we

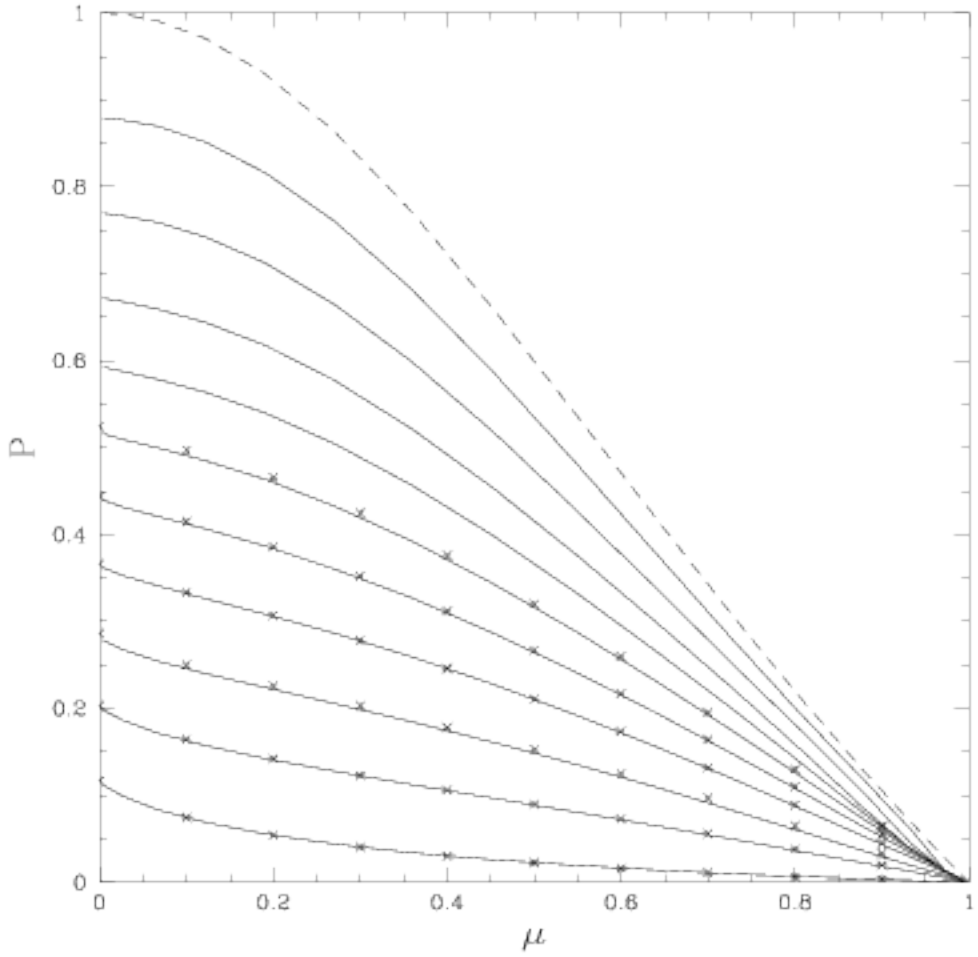

Figure 4.1: Polarization as a function of viewing angle for an unmagnetized ($\delta = 0$) atmosphere with different values of q and all radiation sources at infinite optical depth. From top to bottom, the curves represent the results of our Feautrier calculations for $q = 0.1$ to $q = 1$ in steps of 0.1. Points represent the numerical results of Loskutov and Sobolev (1979), which are consistent with our results. The dashed line represents our analytic solution for $q \to 0$, equation 4.6.

again confirm this fact. Physically this is somewhat puzzling, because it suggests that the polarization remains finite even in the $q \to 0$ limit where there is no scattering opacity.

We have obtained the following $q \to 0$ analytic solution to this problem in the unmagnetized case. For outward rays ($0 \leq \mu \leq 1$),

$$I(\tau, \mu) = \frac{(1+\mu^2)e^{\tau}}{(1-\mu)e^{4/3q}+2} I(0,1), \tag{4.2}$$

and

$$Q(\tau, \mu) = (1+\mu)e^{\tau - 4/3q} I(0,1). \tag{4.3}$$

For inward rays ($-1 \leq \mu < 0$),

$$I(\tau, \mu) = \frac{(1+\mu^2)(e^{\tau} - e^{\tau/\mu})}{(1-\mu)} e^{-4/3q} I(0,1), \tag{4.4}$$

and

$$Q(\tau, \mu) = (1+\mu)(e^{\tau} - e^{\tau/\mu})e^{-4/3q} I(0,1). \tag{4.5}$$

The Stokes parameter U vanishes because $\delta = 0$. This solution may be verified directly by substitution in equation (2.26). In this limit the emergent intensity vanishes except in the upward vertical direction ($\mu = 1$), i.e. there is absolute limb darkening. The polarized flux which is represented by Q vanishes for all viewing angles, consistent with the fact that there is no scattering opacity. The degree of polarization does not vanish, however, except along the vertical ($\mu = 1$) because of symmetry:

$$P = \frac{Q}{I} = \frac{1-\mu^2}{1+\mu^2}. \tag{4.6}$$

This polarization is also plotted in figure 4.1 as the dashed line.

For magnetized atmospheres with finite δ, equations (4.2)-(4.6) still represent the solution for the radiation field in the $q \to 0$ limit. This is because the Faraday rotation term in equation (2.24) is proportional to q. In other words, Faraday rotation depends on the electron density, and therefore must have negligible effect when absorption dominates over electron scattering. This is true even though this electron scattering produces a nonzero degree of polarization.

Figure 4.2 shows the polarization for $q = 0.8$ and $q = 0.2$ atmospheres with various magnetic field strengths represented by δ. As expected, Faraday rotation

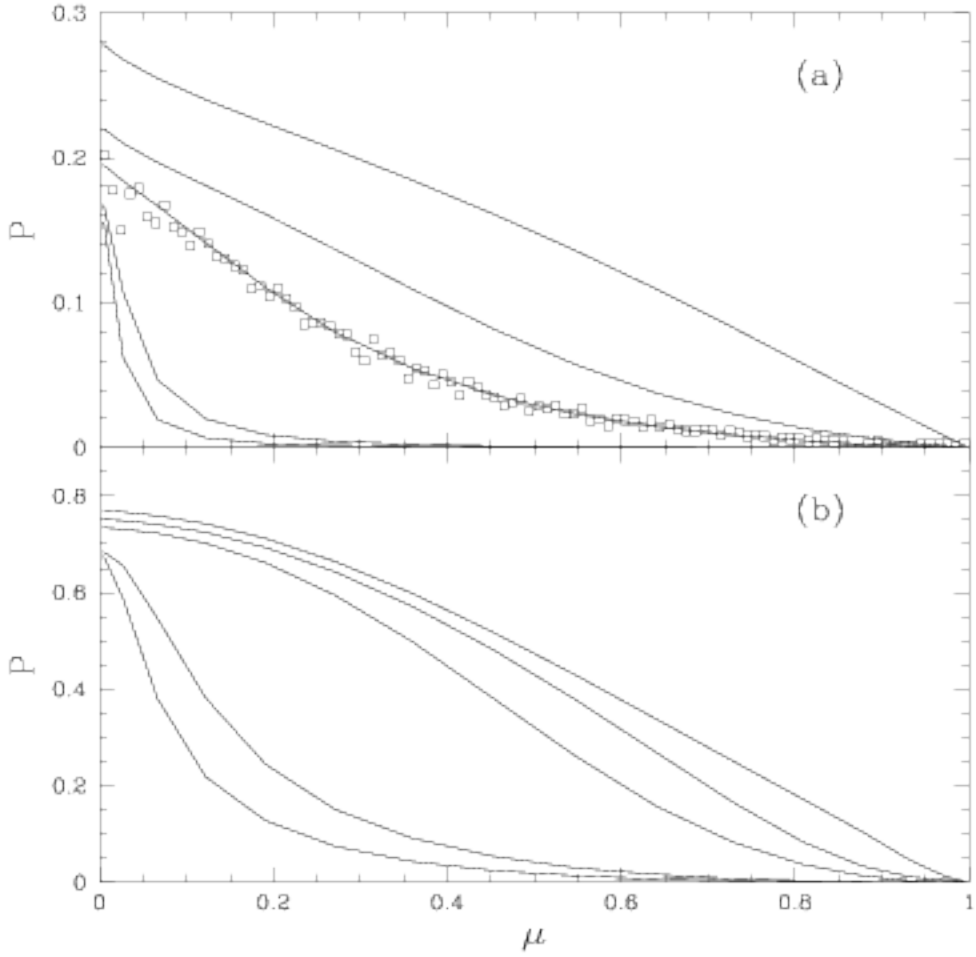

Figure 4.2: Polarization as a function of viewing angle for (a) $q = 0.8$ and (b) $q = 0.2$ atmospheres with various values of δ and all radiation sources at infinite optical depth. From top to bottom, the curves represent the results of our Feautrier calculations for $\delta = 0$ (i.e. zero magnetic field), 2, 5, 50, and 100. Square points represent the results of our Monte Carlo calculations for the case $q = 0.8$ and $\delta = 5$, and confirm the Feautrier results.

depolarizes the radiation field. This figure should be compared to figure 2(b) of chapter 2 which shows the same thing for a $q = 1$ (zero absorption, pure electron scattering) atmosphere. It is apparent that moderate absorption opacity (e.g. $q = 0.8$) *enhances* the depolarizing effects of the magnetic field, even though the electron scattering depth down to unit optical depth is smaller. This is true even along lines of sight which are perpendicular to the magnetic field ($\mu = 0$).

Faraday rotation generally has only a very small effect on the limb darkening of the total intensity of the radiation field emerging from an atmosphere, as shown in figure 4.3. In the pure scattering, $q = 1$ case, large Faraday rotation acts to randomize a photon's polarization vector between scatterings, and the limb darkening law approaches that for scattering described by Rayleigh's phase function (cf. the appendix and section 45 of Chandrasekhar 1960), i.e. Thomson scattering of unpolarized radiation. This limb darkening law turns out to be very close to the pure electron scattering case with polarization effects. As shown by the $q = 0.8$ curves in figure 4.3, modest absorption causes Faraday rotation to have a more substantial effect on the limb darkening, although it is still small. This is because the polarization is greater than for the $q = 1$ case. The contribution of Q to the intensity source function is therefore larger, so as the magnetic field depolarizes, the intensity source function is modified more than for the $q = 1$ case. For large absorption opacity, e.g. the $q = 0.2$ case shown in figure 4.3, the effects of Faraday rotation are very small.

Figure 4.4 shows the depolarizing effects of Faraday rotation for all values of q. Overall, as q decreases below unity, Faraday rotation is at first more effective in depolarizing the radiation field than at $q = 1$. The polarized source function has a greater contribution from Q relative to I than it did in the $q = 1$ case. The limb darkening does not change much with δ, so as the Faraday rotation is added and the polarization is reduced (except for μ near 0), the polarized source function for $\mu = 0$ decreases more rapidly than in the $q = 1$ case. However, as q gets below around 0.4 for the particular viewing angle shown in figure 4.4, Faraday rotation starts to become less effective in depolarizing the radiation field compared to the $q = 1$ case because of the diminishing electron column density down to unit optical depth. As $q \to 0$, Faraday rotation has zero effect as we noted in our analytic solution above.

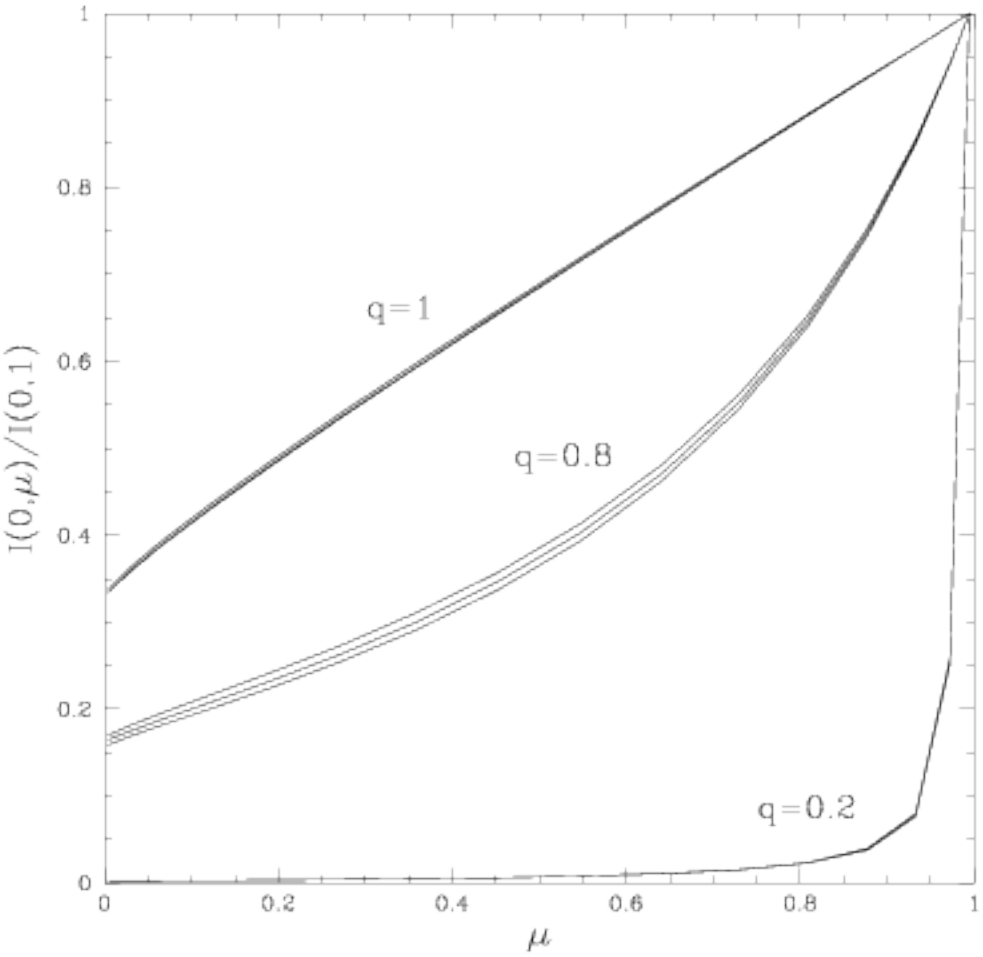

Figure 4.3: Angular distribution of total intensity I emerging from atmospheres with $q = 0.2$, $q = 0.8$, and $q = 1$; $\delta = 0$, 2, and 100; and all radiation sources at infinite optical depth. In the $q = 0.2$ and $q = 1$ cases the limb darkening is virtually independent of δ, and the three curves in each case lie nearly on top of each other. In the $q = 0.8$ case, δ increases from bottom to top. All curves were calculated using our Feautrier code. Note that for small q, the limb darkening becomes very large, in agreement with equation (4.2).

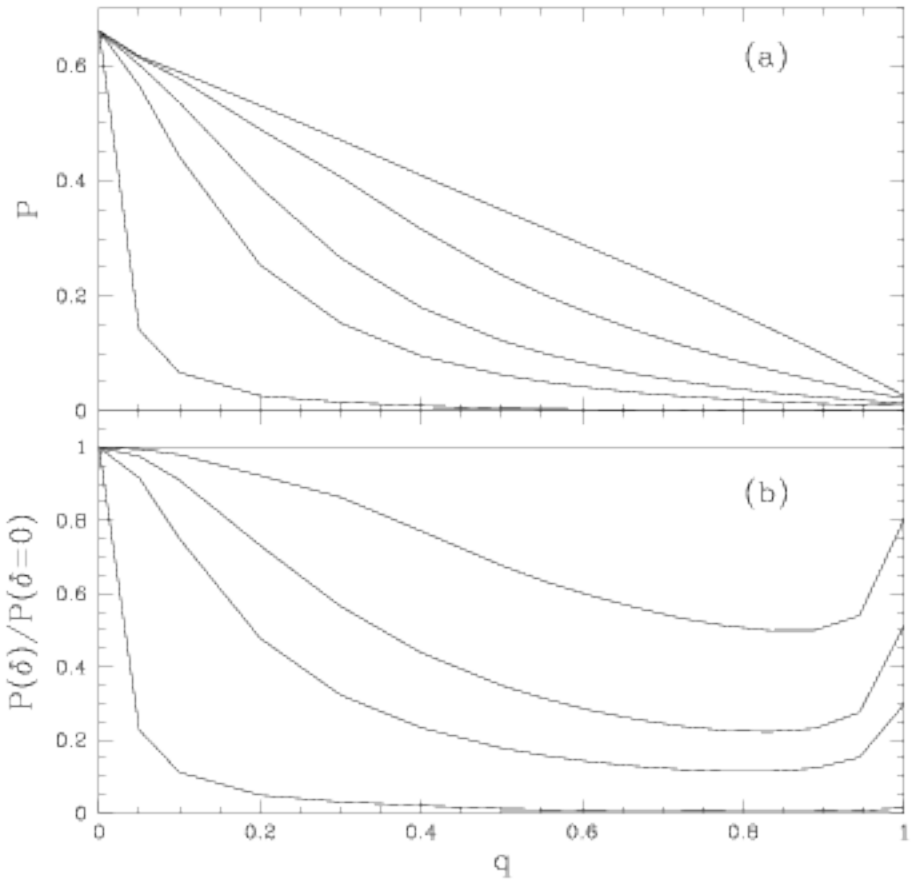

Figure 4.4: Polarization as a function of q along the $\mu = 0.452$ line of sight for various values of Faraday rotation parameter δ. In (a) we show the actual polarization, while in (b) we show the ratio of the polarization to that of the $\delta = 0$ (unmagnetized) case. From top to bottom in both figures, the curves represent $\delta = 0$, 2, 5, 10, and 100. All the results shown were calculated using our Feautrier code.

4.3.2 Case 2: linear thermal source function

We now consider a distribution of sources in the atmosphere such that the thermal source function depends linearly on optical depth,

$$S(\tau) = S(0)(1 + \beta\tau), \tag{4.7}$$

where $S(0)$ and β are constants. In the $q \to 1$ limit, this problem reduces again to the pure electron scattering case considered in chapter 2.[1] We use the diffusion approximation to apply a lower boundary condition at sufficiently high optical depth $\tau_{\rm max}$ so that the results are independent of $\tau_{\rm max}$. Apart from the uninteresting normalization factor, the radiation field emerging from this atmosphere now depends on three parameters: δ, q, and β.

For atmospheres with very small scattering opacities ($q \to 0$), the radiative transfer equation may be solved perturbatively. To lowest order in q, the total intensity from the atmosphere is given by the Eddington-Barbier relation,

$$I(0, \mu) = S(0)(1 + \beta\mu) + O(q), \tag{4.8}$$

and the polarization is given by

$$P(\mu) = q\frac{3(1-\mu^2)}{16(1+\beta\mu)}\left\{\mu\Phi(\mu) + \beta\left[\frac{1}{4} + \mu^2\Phi(\mu)\right]\right\} + O(q^2), \tag{4.9}$$

where

$$\Phi(\mu) \equiv \frac{3}{2} - 3\mu + (3\mu^2 - 1)\ln\left(1 + \frac{1}{\mu}\right). \tag{4.10}$$

These results are identical to those obtained by Gnedin and Silant'ev (1978) for unmagnetized atmospheres in the $q \to 0$ limit, and this is because the effects of Faraday rotation are of order q^2 in this limit. Physically, the ratio of scattered to thermal (unpolarized) intensity is of order q, which is why the polarization is also of this order. (This is in marked contrast to the previous case we considered where the thermal sources were all at infinite optical depth. Here the presence of a nonzero thermal source function ensures that the polarization vanishes as $q \to 0$.) The amount by which Faraday rotation can further depolarize the

[1] This is true provided the thermal source function remains finite. By $q \to 1$, we mean that $n_e\sigma_T \gg \kappa$ and that the scattering source function is much larger than the thermal source function.

radiation is also of order q, because this is the factor by which the electron column density (which does the rotation) down to unit optical depth is reduced. Hence we immediately conclude again that Faraday rotation has negligible effect on the polarization (which is already small) as $q \to 0$.

Figure 4.5 shows the polarization viewed along $\mu = 0.452$ for various values of β and q for an unmagnetized atmosphere.[2] Also shown are the numerical results of Loskutov and Sobolev (1979), which are again in good agreement with ours. Negative values of P in this figure represent cases where the polarization plane is perpendicular to the plane of the atmosphere. We call this the "Nagirner effect", after the person who first noted that absorption opacity can produce this (cf. Gnedin and Silant'ev 1978). It is possible that this effect could explain the fact that the observed polarization in type I AGN is parallel to the radio axis. We find that negative polarization is present for some μ and q if and only if $\beta < (6 - 8\ln 2)/(8\ln 2 - 5) = 0.834$. This is consistent with Gnedin and Silant'ev (1978) $q \to 0$ result, because as β drops below the critical value, Q first becomes negative for small q.

The Nagirner effect therefore arises for sufficiently flat thermal source functions. It is useful, however, to examine its origin a little more closely by considering the depth dependence of the *total* source function. If there is no magnetic field, then the outgoing radiation ($0 \le \mu \le 1$) can be formally expressed from equation (2.26) as

$$\mathbf{I}(0,\mu) = \int_0^\infty \mathfrak{F}(t,\mu) e^{-t/\mu} \frac{dt}{\mu}. \tag{4.11}$$

Hence if $\mathfrak{I}_Q(\tau,\mu) < 0$ over some range of optical depths, then the outgoing radiation can be negatively polarized for that particular viewing angle. The solid curve in figure 4.6 shows the depth dependence of $\mathfrak{I}_Q(\tau)$ for $\beta = 0$, $q = 0.8$, and $\mu = 0.211$. Around $\tau = 1$, $\mathfrak{I}_Q$ is negative, but for low τ it becomes positive. The reason for this can be seen by looking at the contribution to the polarized source function from radiation coming from different directions in an atmosphere with constant source function. The broken curves in figure 4.6 show the contribution to the source function from different angles in a four-stream calculation of the radiation field, i.e. where the radiation is calculated at four angles for the purposes of computing quadratures. Near $\tau = 0$, there is no downgoing radiation ($\mu < 0$), so the only contribution is from upgoing radiation. The limb darkening causes the source function polarization to be positive, since the

[2]The $\beta = \infty$ case corresponds to $S(\tau) \propto \tau$.

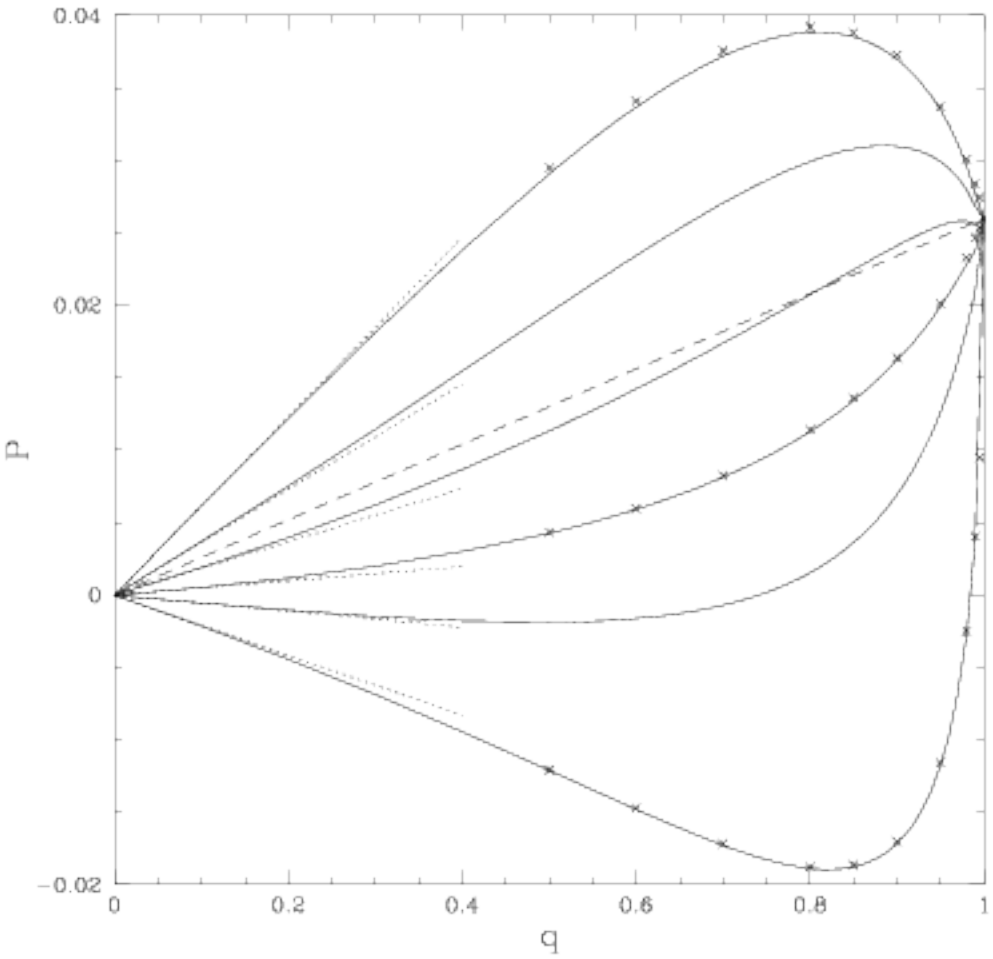

Figure 4.5: Polarization as a function of q along the $\mu = 0.452$ line of sight for various values of source function gradient β in an unmagnetized ($\delta = 0$) atmosphere. From bottom to top, the curves represent the results of our Feautrier calculations for $\beta = 0$, 0.5, 1, 2, 5, and ∞. Points represent the numerical calculations of Loskutov and Sobolev (1979), interpolated to $\mu = 0.452$. The dotted lines are the results of the analytic formula for small q, equation (4.9). The dashed line is the approximation used by Laor et al. (1990). All curves approach the Chandrasekhar (1960) value for this viewing angle as $q \to 1$.

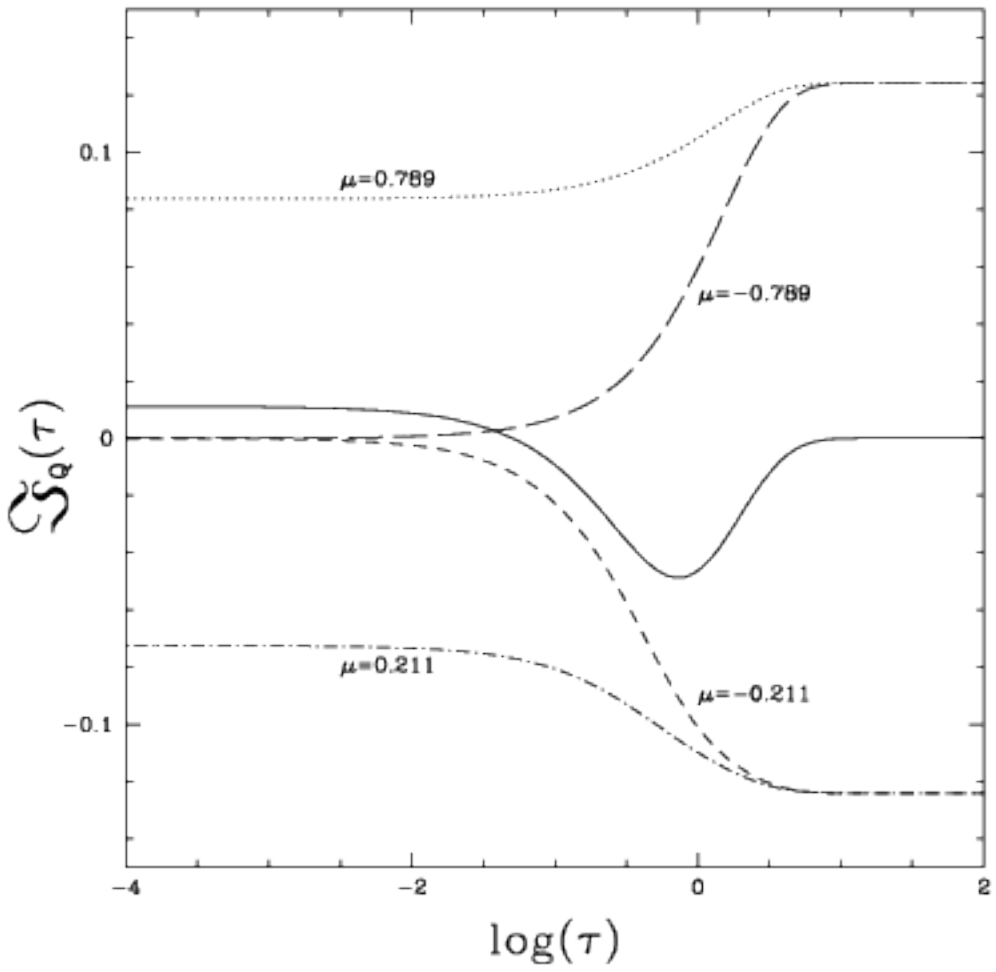

Figure 4.6: Polarized source function vs. optical depth along the $\mu = 0.211$ line of sight for $\beta = 0$ and $q = 0.8$. The solid curve is the total source function, while the dashed and dotted curves are the contributions from various angles in the four-stream approximation (negative μ is downwards). The plot of $\Im_Q(\tau)$ for the $\mu = 0.789$ line of sight is very similar.

near-vertical radiation (which has net positive polarization when scattered) is stronger than the near-horizontal radiation (which has net negative polarization when scattered). Near $\tau = 1$, the limb darkening is weaker. Here, there begins to be a significant contribution to the source function from downward radiation which is produced in the layers above $\tau = 1$. The near-horizontal radiation is stronger than the near-vertical since there is more atmosphere emitting from smaller $|\mu|$. This leads to a net negative polarization at $\tau = 1$. Figures 4.7 and 4.8 illustrate this effect. (Note that the polarization is low, so most of the contribution to $\Im_Q$ comes from I. Thus, the corresponding difference in the contribution to $\Im_Q$ from different angles is due mostly to the difference in the intensities from different angles.) When the thermal source function has a steep vertical gradient, the limb darkening is stronger. The contribution from the downward going radiation is less than that of the upward radiation, and the polarization source function is always positive. This is why flat thermal source function gradients are required for the Nagirner effect to be present.

Figure 4.9 shows the polarization as a function of viewing angle for $\beta = 1$ and (a) $q = 0.8$ and (b) $q = 0.2$. This figure should be compared with figure 4.2 above. Faraday rotation has a much smaller effect on the polarization at $\mu = 0$ when a nonzero thermal source function is present. This is because the polarization is low and limb darkening is more important in determining the polarized source function. In addition, the presence of the thermal source function implies that the overall polarization vanishes as $q \to 0$. Faraday rotation has even less effect on the polarization, which is already small, as $q \to 0$. For example, in the $q = 0.2$ case shown in figure 4.9(b), the $\delta = 0$, 2, and 5 curves overlap because the effects of Faraday rotation are reduced by an additional factor of q as discussed above.

Figure 4.10 shows the polarization in the $\beta = 1$ and ∞ cases as a function of q for various δ. Notice again that as q becomes small, the effect of the Faraday rotation decreases, and all curves approach the $\delta = 0$ case. Note however that this approach is much smoother than in the previous case where all the sources were at infinite optical depth (cf. figure 4.4). For moderate absorption opacity (q slightly less than unity), the depolarizing effects of Faraday rotation are again enhanced over the pure scattering problem for the $\beta = \infty$ case shown. This is the same effect as in section 3.1, and again arises because the absorption opacity on its own increases the polarization. If the thermal source function gradient is not so steep so that modest absorption opacity decreases the polarization, then the effects of Faraday rotation are reduced as q drops below unity (cf. the $\beta = 1$

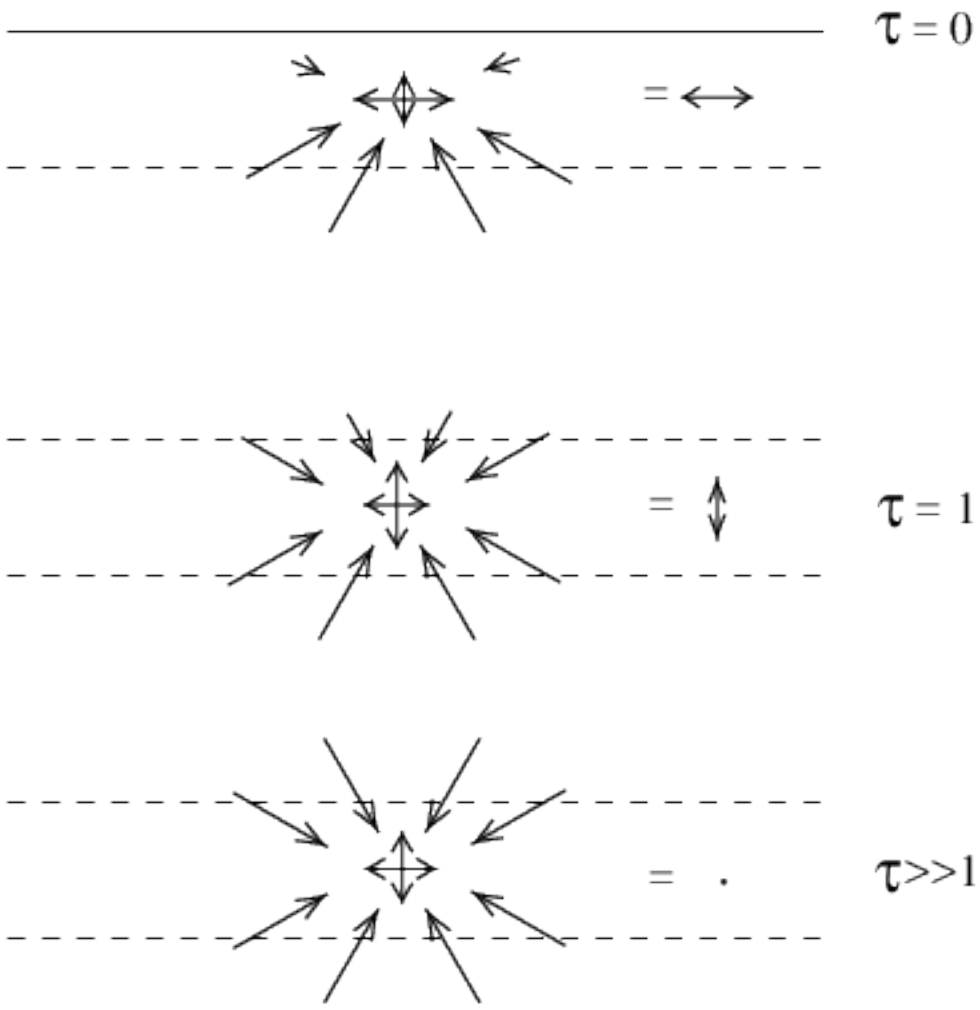

Figure 4.7: Cartoon showing the reason why the polarized source function switches from positive to negative to zero with increasing τ. The length of the radial arrows represents the strength of radiation coming from different angles. The arrows in the center represent the strength of the negative and positive contributions to the polarized scattering source function (negative is vertical, positive is horizontal). The sum of the polarizations is indicated on the right, along with the optical depth of each layer.

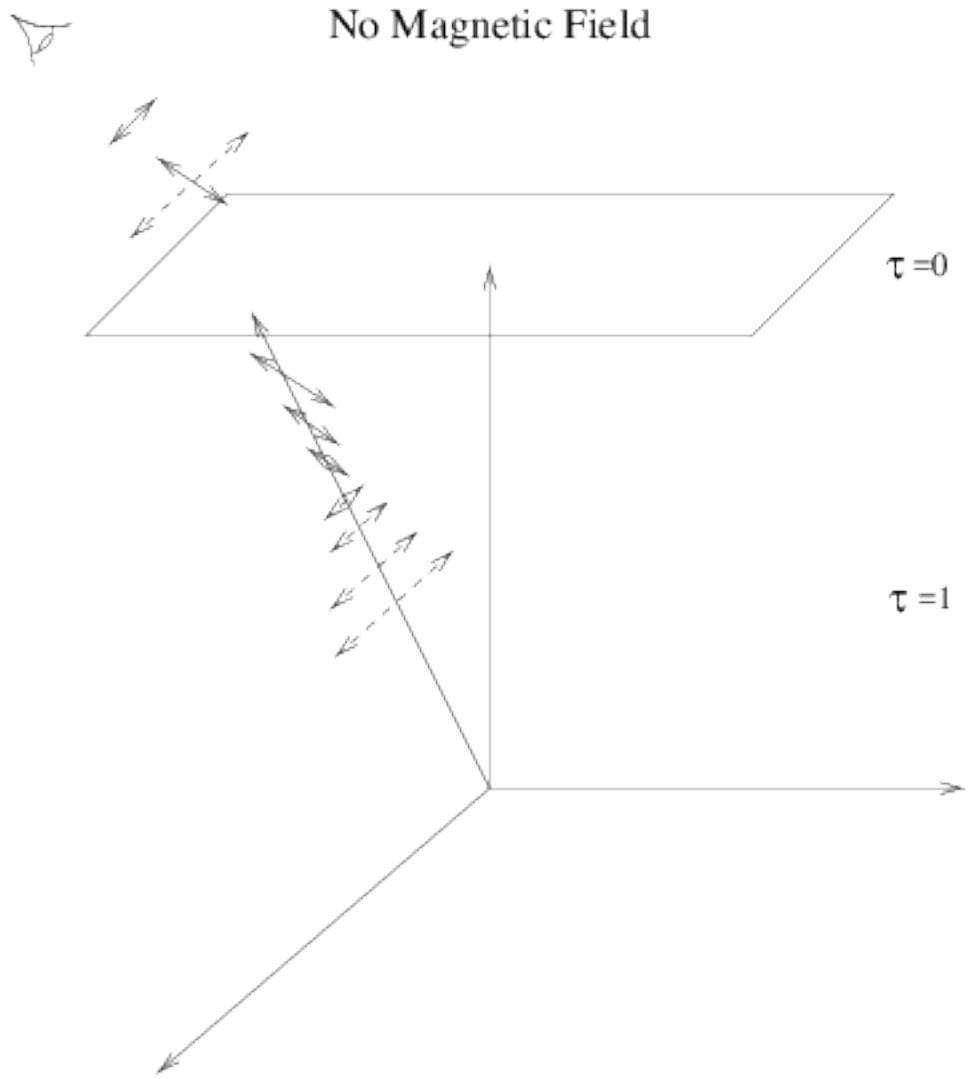

Figure 4.8: At wavelengths where the Nagirner effect is present, the polarization vector lies in the plane of the line of sight and the vertical at $\tau = 1$, while it is perpendicular near $\tau = 0$. Thus, the polarization ends up being negative at some viewing angles. However, when a magnetic field is added, Faraday rotation causes the polarization near $\tau = 1$ to be rotated and depolarized, while the radiation near $\tau = 0$ is rotated very little, so the polarization ends up being nearly perpendicular.

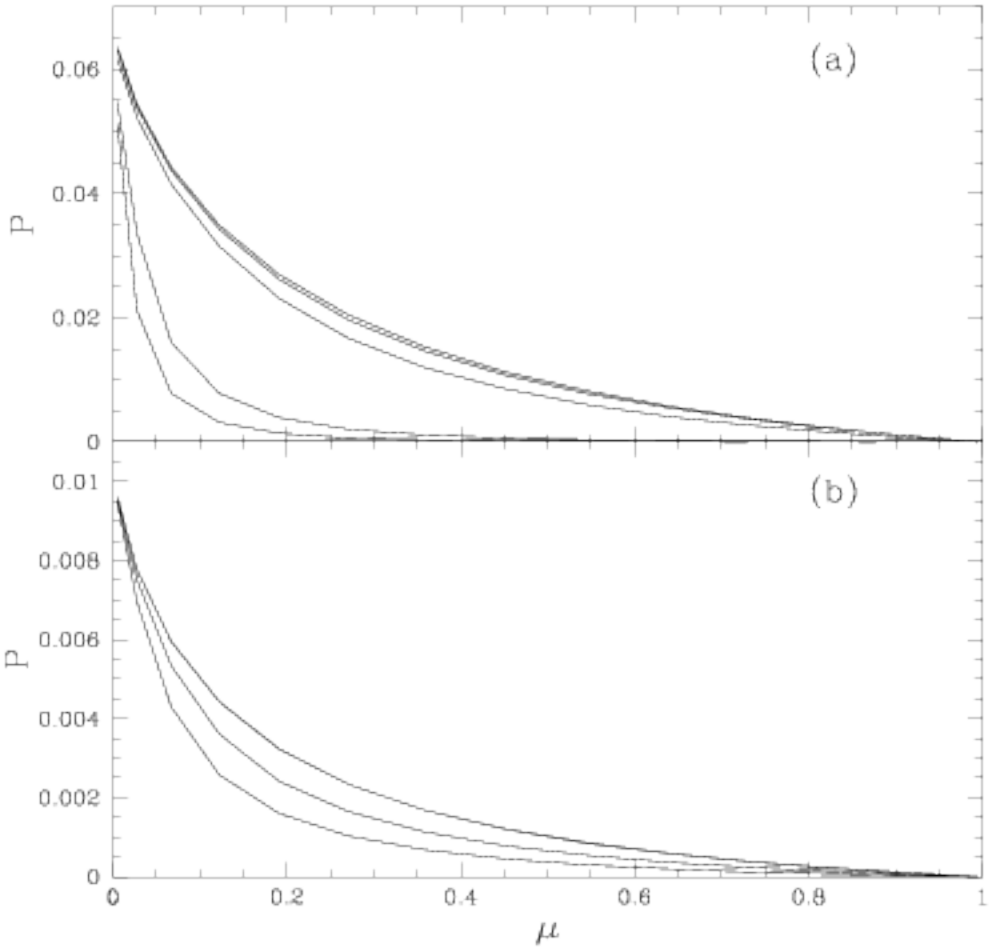

Figure 4.9: Polarization as a function of viewing angle for (a) $q = 0.8$ and (b) $q = 0.2$ atmospheres with various values of δ and a linear source function with $\beta = 1$. From top to bottom, the curves represent the results of our Feautrier calculations for $\delta = 0$, 2, 5, 50, and 100. In panel (b), the δ= 0, 2, and 5 cases overlap.

case in figure 4.10).

So far we have discussed Faraday rotation as an agent for depolarizing the radiation field. However, when β is small and the Nagirner effect is present, it is possible for the magnetic field to *increase* the polarization. Figure 4.11 shows the normalized Stokes parameters for $q = 0.9$ and $\beta = 0.25$ for various δ, and Q/I with the $\delta = 0$ case subtracted. With no magnetic field, the $\Im_Q$'s from different depths partially cancel, making the polarization negative for $\mu > 0.38$, but positive for smaller μ.

Since $\Im_U = 0$, the only contribution to the polarization is from $\Im_Q$, which for $q = 0.9$ and $\beta = 0.25$ is similar to the source function plotted in figure 4.6. Because the polarization is low, $\Im_Q$ does not change much with δ here. For this case, $\Im_Q < 0$ for $\tau > 0.25$ at all μ. Thus, the positive polarized source function comes from a small range of electron scattering depths, so the Faraday depolarization is insignificant for $\delta \lesssim 4$. However, the negative polarized source function comes from a larger range of optical depths, causing Faraday depolarization for $\delta \simeq 1$, reducing the magnitude of the negative polarization so that the outgoing polarized flux is increased.[3] For very large δ, even the radiation from small τ will be Faraday rotated significantly, so the polarization will still be approximately horizontal, but will eventually start to decrease in magnitude again, as seen in figure 4.11. The effect of increasing the polarization with increased magnetic field in a semi-infinite atmosphere is only present when there is absorption opacity present and a shallow source function gradient.

4.4 Polarization from realistic accretion disk atmospheres

In chapter 3 we calculated the structure of local, static, plane-parallel atmospheres using the complete linearization technique, neglecting the effects of any

[3]Strictly speaking, "positive" and "negative" polarization define the orientation of the plane of polarization only when there is no magnetic field present, because there are only two possible orientations. The presence of the magnetic field breaks the azimuthal symmetry and allows the plane of polarization to be at an arbitrary angle with respect to the vertical/line of sight plane. We use these terms here in reference to the unmagnetized case to show how Faraday rotation acts on the different orientations of the polarization at different depths in the atmosphere.

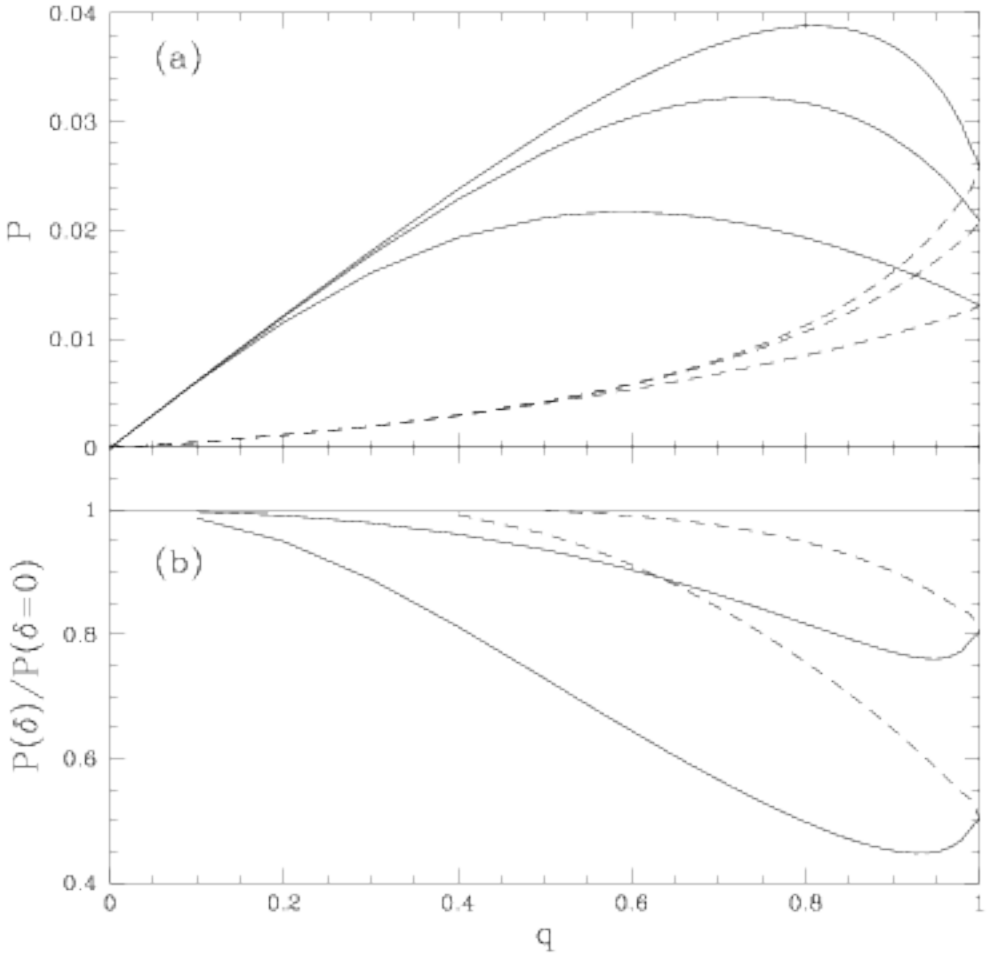

Figure 4.10: The effect of Faraday rotation on the β= 1 (dashed) and ∞ (solid) cases for the $\mu = 0.452$ line of sight. In (a) we show the actual polarization, while in (b) we show the ratio of the polarization to that of the $\delta = 0$ (unmagnetized) case. From top to bottom in both figures, the curves represent the results of our Feautrier calculations for $\delta = 0$, 2, and 5.

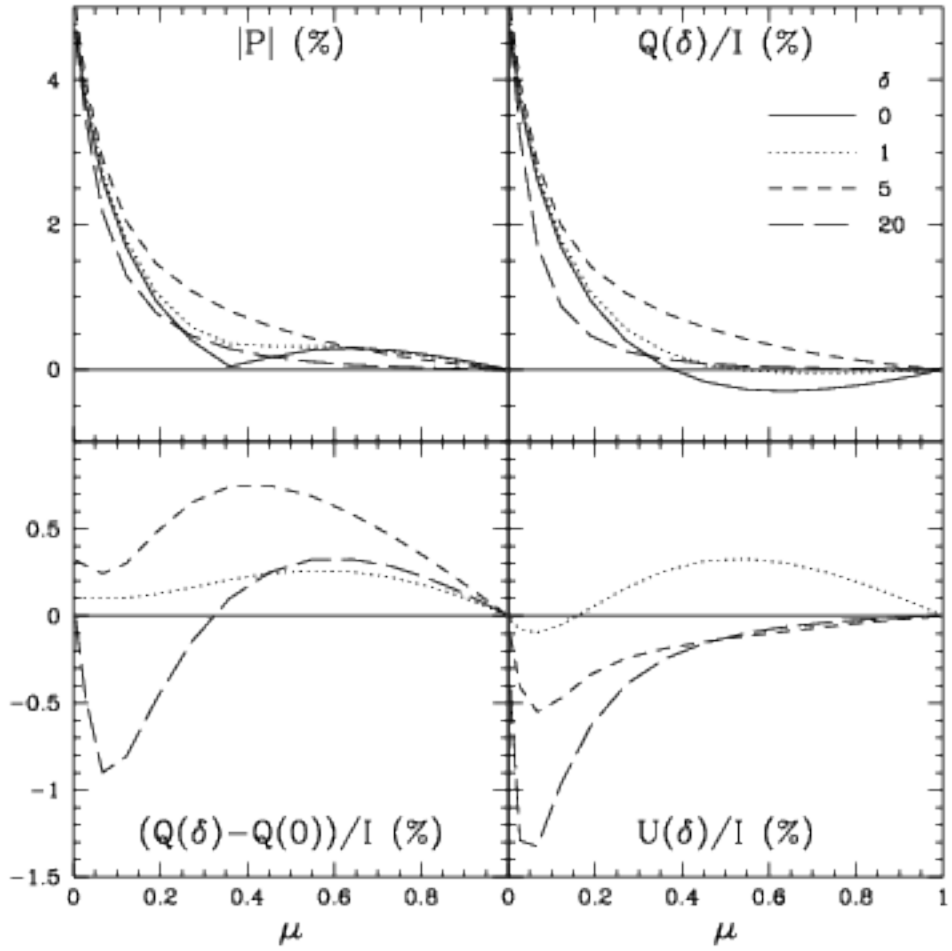

Figure 4.11: The top panel shows P and Q/I, and the bottom panel $(Q(\delta) - Q(0))/I$ and U/I as δ increases in an atmosphere with $q = 0.9$ and $\beta = 0.25$. Note that at large δ and small μ, Q/I decreases relative to the zero magnetic field case, which is because the Faraday rotation is significant for small optical depths when δ is large enough.

magnetic field.[4] Here we use some of these atmospheres to calculate the radiative transfer in the presence of a constant vertical magnetic field in the atmosphere according to equation (2.24). Our atmosphere solutions include hydrogen bound-free and free-free opacities as well as electron scattering opacity. Non-LTE effects in the $n = 1$ and 2 levels of hydrogen are included. The results with magnetic fields of different strengths in atmospheres with (T_{eff}, g) of (2×10^4 K, 190 cm s^{-2}), (4.5×10^4 K, 4×10^3 cm s^{-2}), and (10^5 K, 9.5×10^4 cm s^{-2}) are plotted in figures 4.12-4.14, respectively. We also show the variation of q at $\tau = 1$ with wavelength in figure 16 for these three atmospheres. In all cases the magnetic field does not significantly affect the total intensity spectrum I_λ.

As shown in figure 4.15, q is very small just blueward of the Lyman edge, so the Faraday rotation does not affect the polarization very much in this region of the spectrum unless δ is very large. This is illustrated in figures 4.12-4.14. In the case shown in figure 4.12, the source function is shallow just blueward of the Balmer edge. Hence $\Im_Q < 0$ near $\tau = 1$ at these wavelengths. Here the increasing magnetic field causes an *increase* in polarization, as described in section 3. Figure 4.12 also shows a dramatic reduction in the difference in polarization across the Lyman edge. This is due to the fact that redward of the edge, q_ν is large, so the Faraday depolarization is strong. Blueward of the edge, however, q_ν is small, so the Faraday depolarization is weak. Thus, as the magnetic field increases, the polarization decreases faster redward than blueward of the edge. In some cases the polarization blueward of the edge is larger than redward of the edge, as shown in figure 4.14 for $B = 2500$ G.

The Balmer edge in figure 4.13 has a negative polarization, which becomes more negative redward of the edge for $B = 0$. However, as the magnetic field increases, the polarization first becomes positive, and increases from blue to red across the edge. For larger B, the polarization is reduced, decreasing from blue to red. This behavior can be understood in terms of the physics discussed in section 3. The thermal source functions are very flat on both sides of the Balmer edge, but q is larger redward of the edge ($q \simeq 0.8$ at $\tau = 1$) than blueward of the edge ($q \simeq 0.57$ at $\tau = 1$). Hence the Nagirner effect is stronger (cf. figure 4.5). Since Faraday depolarization is stronger for larger q, the polarization increases to the red across the edge when there is a 20 G magnetic field ($\delta = 2.1$ at 3648Å). However, when δ is larger, the depolarization is more rapid for larger

[4] In particular, we ignore the contribution of magnetic field pressure on hydrostatic equilibrium, which is quite important for equipartition fields.

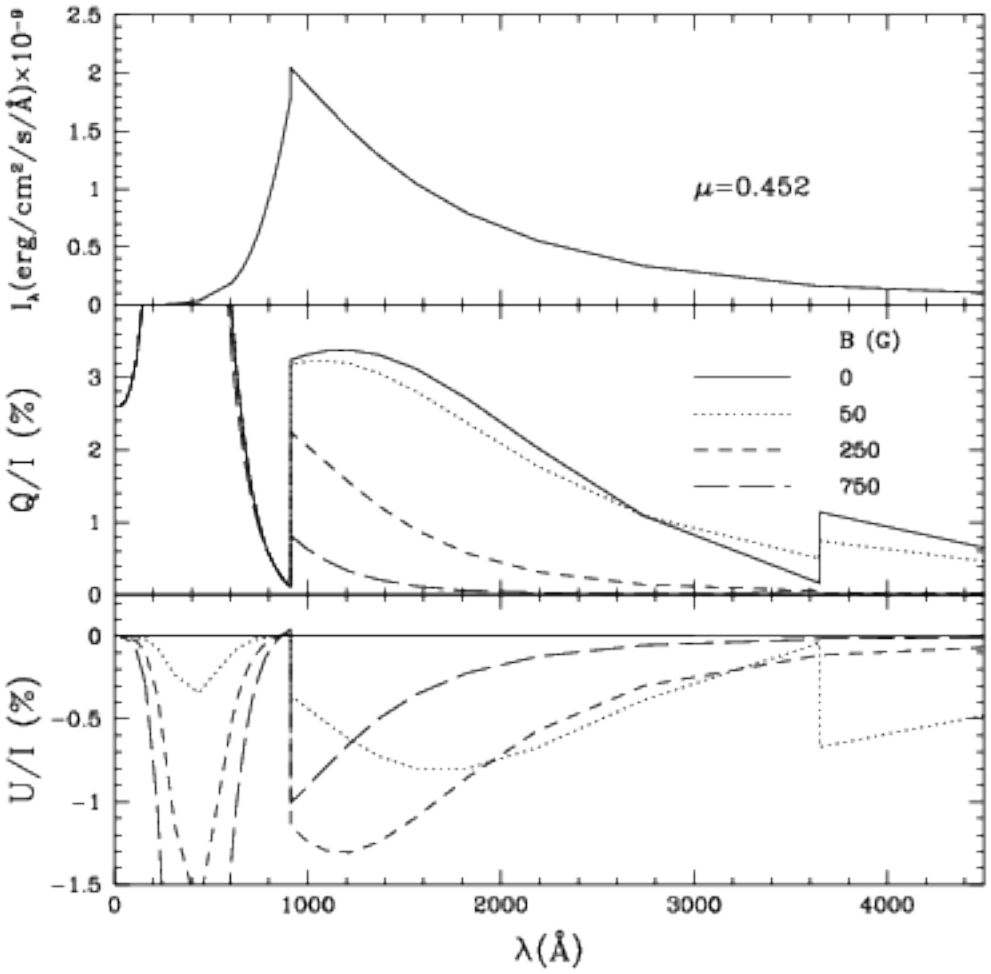

Figure 4.12: Stokes parameters in an atmosphere including Faraday rotation for $T_{eff} = 20,000$ K and $g = 190$ cm s^{-2} including non-LTE effects for two hydrogen levels. The curves depicted are for a $\mu = 0.452$ line of sight, with various magnetic field strengths. The top panel shows the outgoing total intensity spectrum $I_\lambda = \nu/\lambda I_\nu$. The bottom two panels show the percent polarization for the Q/I and U/I Stokes parameters. Q/I peaks at 10 per cent and U/I peaks at -4 per cent at about 500Å for $B = 750$ G. If the magnetic field is in equipartition with the radiation field, $B_{eq} = 174$ G.

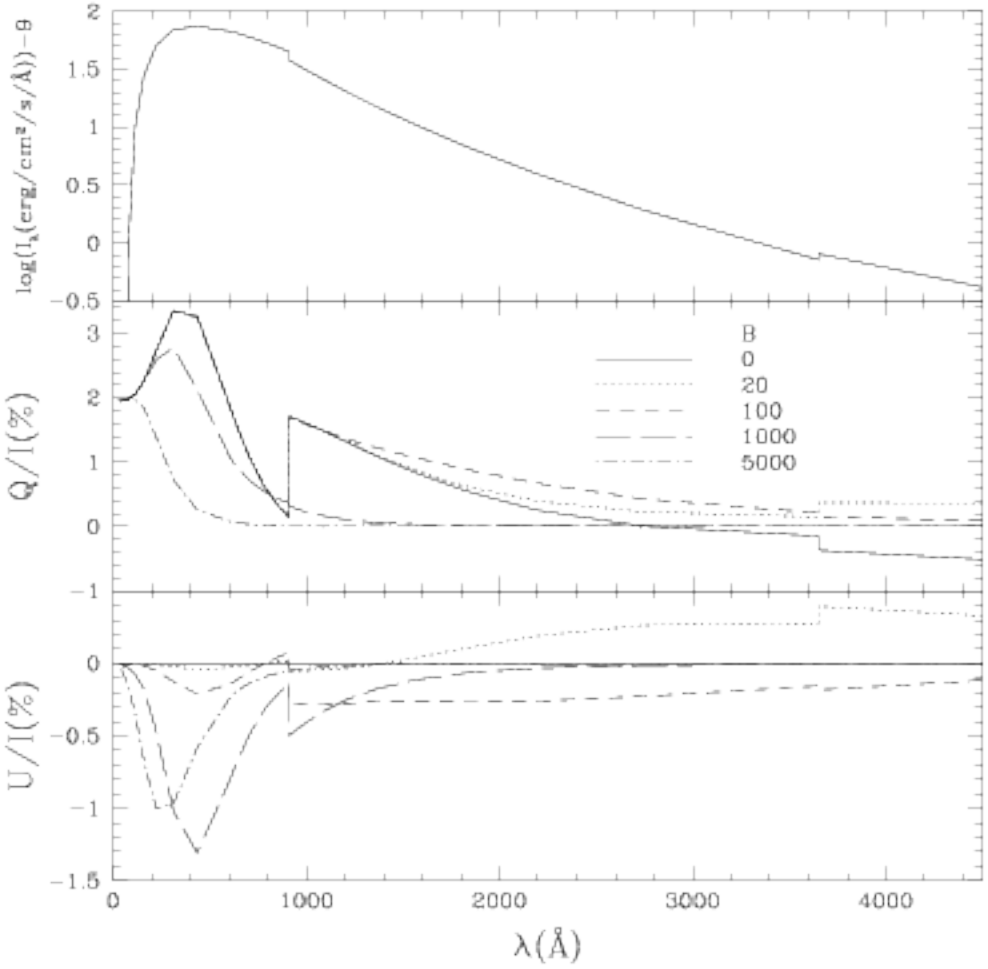

Figure 4.13: Polarization in an atmosphere including Faraday rotation for $T_{eff} = 45,000$K, $g = 4000$ cm s^{-2}, and $\mu = 0.55$ and various magnetic field strengths. If the magnetic field is in equipartition with the radiation field, $B_{eq} = 880$ G.

q, so then the polarization decreases to the red across the edge when $B = 100$ G, or $\delta = 10.5$ at 3648Å.

If the magnetic field were randomly oriented, the polarization feature may also be decreased at larger inclination angles for a large magnetic field.

The results of this section are meant to give a flavor of the complexities that may result in the polarized spectrum emerging from a realistic atmosphere. The full accretion disk spectrum requires an integration over many such atmospheres in different physical conditions representing the disk at different radii.

4.5 Conclusions

Using a combination of numerical calculations and analytic arguments, we have extended our study of Faraday rotation in accretion disk atmospheres to include the interaction with absorption opacity. Along the way we have clarified the role that each of these two effects play separately. Faraday rotation in a pure electron scattering atmosphere acts to depolarize the radiation field by rotating the polarization vectors of photons scattered from different depths.

Absorption opacity in an unmagnetized atmosphere can increase or decrease the polarization depending on the behavior of the thermal source function. If the thermal source function is zero except at great depth, absorption opacity alone always increases the polarization. In the more usual case of nonvanishing thermal source function, the effect of absorption opacity depends on the source function gradient. If the thermal source function increases steeply with depth, absorption opacity can increase the polarization over the pure electron scattering case. On the other hand if the source function increases slowly with depth, or even decreases, then absorption opacity can flip the plane of polarization to be in the vertical/line of sight plane. While these results were known from previous work (Gnedin and Silant'ev 1978; Loskutov and Sobolev 1979), we have presented a novel physical interpretation in terms of the behavior of the total source function $\mathfrak{S}$. Quite generally this source function locally produces polarization which is parallel to the atmosphere plane at low optical depths. At optical depths around unity, however, the polarization can be parallel or perpendicular to the atmosphere plane depending on the thermal source function gradient.

When Faraday rotation is combined with absorption opacity in a scattering atmosphere, a number of effects can occur. First, if absorption dominates

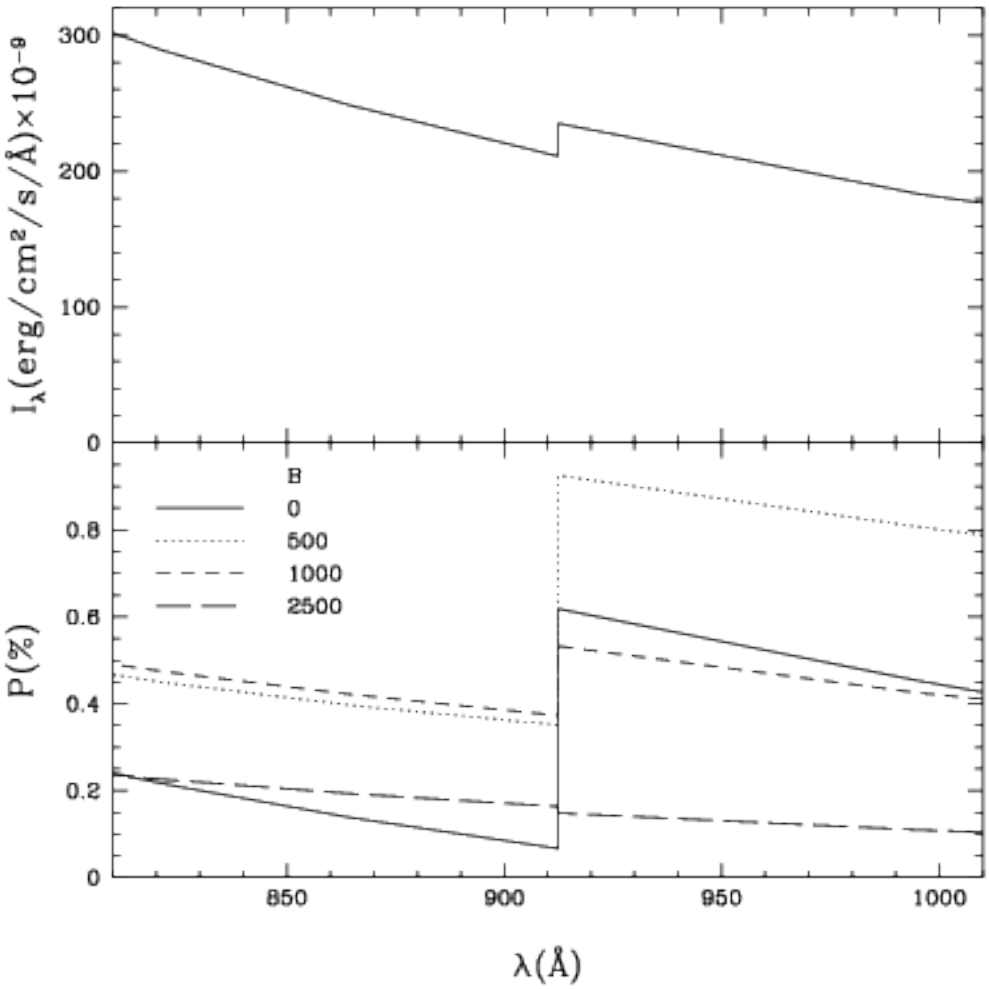

Figure 4.14: Polarization near the Lyman edge in an atmosphere including Faraday rotation for $T_{eff} = 100,000$ K, $g = 95,000$ cm s^{-2}, and $\mu = 0.55$ and various magnetic field strengths. If the magnetic field is in equipartition with the radiation field, $B_{eq} = 4400$ G.

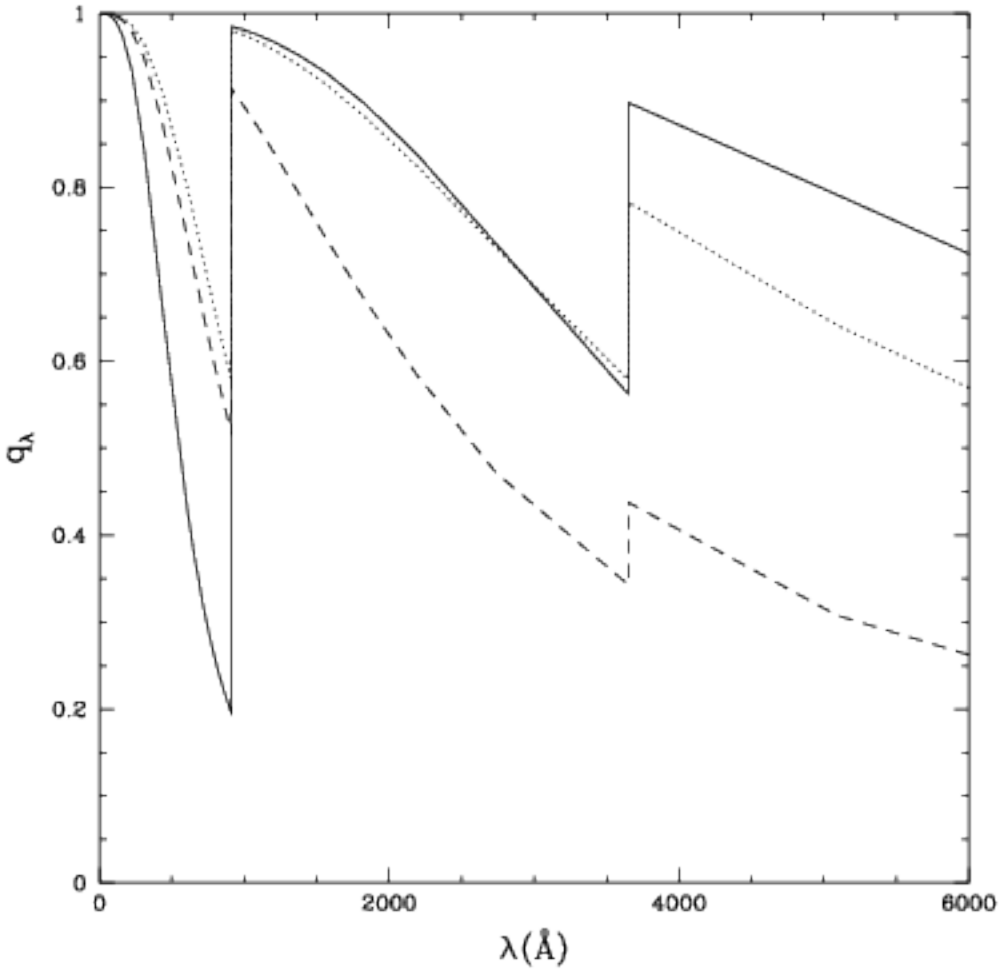

Figure 4.15: The ratio of scattering opacity to total opacity at $\tau = 1$ for the three atmospheres displayed in figures 13-15. The solid, dotted, and dashed curves represent q_λ for T_{eff}= 20,000K, 45,000K, and 100,000K atmospheres respectively.

scattering, then the electron column density along a photon mean free path is small and Faraday rotation only has a small effect on the polarization of the radiation field. On the other hand, if modest absorption opacity alone increases the polarization, then the depolarizing effects of Faraday rotation are enhanced compared to the pure scattering case, at least for a vertical magnetic field. On the whole Faraday rotation generally acts to depolarize the radiation field, as in the pure scattering case. However, when the Nagirner effect is present at certain photon wavelengths, then Faraday rotation can actually increase the emerging polarization by depolarizing the deeper radiation field which has a perpendicular orientation to the radiation which is scattered from shallower depths.

While we have shown that these effects can all occur in simple toy model atmospheres, we have also demonstrated that they are present in more realistic atmospheres. We have shown how the polarized radiative transfer can be computed in a straightforward manner by a simple extension of the Feautrier method to incorporate a vertical magnetic field. This numerical method can be used to integrate the radiation field produced at different annuli in the accretion disk to calculate the total observed radiation field. As we noted in chapter 2, the largest uncertainty in applying such calculations to the observed data is the variation of magnetic field strength with disk radius, and its covering factor on the disk photosphere. (It might be possible to get a handle on the latter by combining ultraviolet and X-ray observations to determine the "patchiness" of the corona; cf. Haardt, Maraschi, and Ghisellini 1994. This assumes that such patches, if real, are magnetized active regions similar to those on the sun.) The field topology will of course also not be vertical, but following our Monte Carlo work of chapter 2, we expect magnetic fields of random orientation to have qualitatively (and perhaps quantitatively to some extent) similar effects.